

Development of an Electrochemical Ceramic Membrane Bioreactor for the Removal of PPCPs from Wastewater

Kangquan Qi ¹, Mei Chen ¹, Ruobin Dai ¹, Qiang Li ², Miaoju Lai ² and Zhiwei Wang ^{1,3,*}

¹ School of Environmental Science and Engineering, State Key Laboratory of Pollution Control and Resources Reuse, Shanghai Institute of Pollution Control and Ecological Security, Tongji University, Shanghai 200092, China; kangquan19950609@163.com (K.Q.); meichen1228@tongji.edu.cn (M.C.); dairuobin@163.com (R.D.)

² Putuo District Center for Disease Control and Prevention, Shanghai 200333, China; 817125@163.com (Q.L.); lmj982338966@163.com (M.L.)

³ International Joint Research Center for Sustainable Urban Water System, Shanghai 200092, China

* Correspondence: zwwang@tongji.edu.cn; Tel.: +86-21-65975669; Fax: +86-21-65980400

Received: 31 May 2020; Accepted: 22 June 2020; Published: 26 June 2020

Abstract: The removal of pharmaceutical and personal care products (PPCPs) from water and wastewater is of great significance for eco-system safety. In this study, an electrochemical ceramic membrane bioreactor (ECMBR) was developed for removing seven groups (24 kinds in total) of PPCPs from real wastewater. In the presence of an electric field (2 V/cm), the ECMBR could enhance the removal efficiencies for most targeted PPCPs without having adverse impacts on conventional pollutant removal and membrane filtration. The ECMBR achieved higher removal efficiencies for fluoroquinolones (82.8%), β -blockers (24.6%), and sulfonamides (41.0%) compared to the control (CMBR) (52.9%, 4.6%, and 36.4%). For trimethoprim, ECMBR also significantly increased the removal to 66.5% compared to 15.6% in CMBR. Furthermore, the exertion of an electric field did not cause significant changes in microbial communities, suggesting that the enhanced removal of PPCPs should be attributed to the electrochemical oxidation of the built-in electrodes in the ECMBR.

Keywords: pharmaceutical and personal care products; electrochemical membrane bioreactor; advanced oxidation process; membrane filtration; wastewater treatment

1. Introduction

The large quantity of consumed pharmaceutical and personal care products (PPCPs) due to the growth of the world's population, the rapid progress of urbanization, and the outbreak of infectious diseases [1–3] will inevitably lead to the occurrence of them in water and wastewater [4–7]. The persistent existence of PPCPs in the water environment may result in the development of antibiotic-resistant bacteria (ARB) and genes (ARG), causing a potent risk for human health [8,9]. Therefore, the removal of PPCPs from contaminated water is of great significance for the safety of the water eco-system.

Current wastewater treatment plants, mostly employing conventional activated sludge (CAS) processes, are not designed for micropollutant removal and thus could not achieve an efficient removal of PPCPs [10,11]. Membrane bioreactors (MBR), combining membrane separation with biological treatment technology, could enhance PPCP removal due to their high biomass concentration and large sludge retention time [12,13]. However, the removal efficiency is still

unsatisfactory due to the toxicity of PPCPs to microorganisms and the inefficiency of membrane rejection (low molecular weight nature of PPCPs). Therefore, the development of alternative technology is needed for achieving a more efficient removal of PPCPs.

Recently, electrochemical advanced oxidation processes (EAOPs) have attracted much attention for the removal of refractory organic matter [14–18]. The EAOP processes rely on direct electron transfer (DET) or reactive oxygen species (ROS) for pollutant removal [19–21]. However, for real applications major obstacles still exist for EAOP processes: (i) the coexistence of other abundant organic matter significantly affects the removal efficiency of low-concentration PPCPs due to the non-selectivity of ROS; (ii) particulate and colloidal substances can accumulate on the electrodes, thus compromising their electrochemical properties. These inherent drawbacks need to be addressed for their potential applications in real wastewater treatment. Recent studies mainly use synthetic municipal wastewater for investigating the degradation behaviors and mechanisms of PPCPs [21–24]. Reports on the treatment of real wastewater by novel EAOP technologies are scarce.

To solve the drawbacks, we developed an electrochemical ceramic membrane bioreactor (ECMBR) by integrating the EAOP process into an MBR using a ceramic membrane module with built-in electrodes for PPCP removal from real wastewater. We hypothesize that: (i) the microorganisms in the ECMBR could degrade the coexisting biodegradable organic matter and the residual PPCPs would be oxidized by electrochemical oxidation, and (ii) membrane separation could protect the internal electrodes against fouling. The performance of the ECMBR was studied for removing seven groups (24 kinds in total) of PPCPs from real wastewater. Microbial communities were analyzed to identify the potential influence of exerting an electric field on microbial behaviors. Our results demonstrate that the ECMBR has a great potential to be used for PPCP removal from water and wastewater.

2. Materials and Methods

2.1. Chemicals

In total, 7 groups involving 24 kinds of PPCPs were analyzed in this study: (i) sulfonamides (SAs): sulfadiazine (SDZ), sulfathiazole (STZ), sulfamerazine (SMR), sulfamethazine (SMN), sulfamethoxazole (SMX), sulfisoxazole (SFX), sulfamethizole (SML), and sulfadimethoxine (SDM); (ii) fluoroquinolones (FQs): norfloxacin (NOR), ofloxacin (OFL), ciprofloxacin (CIP), enrofloxacin (ENR), and lomefloxacin (LOM); (iii) macrolides (MLs): clarithromycin (CLA), roxithromycin (ROX), tiamulin (TIA), tylosin (TYL), and azithromycin (AZN); (iv) β -blockers: atenolol (ATE), metoprolol (MET), and propranolol (PROP); (v) stimulants: caffeine (CAF); (vi) dihydrofolate reductase inhibitors: trimethoprim (TMP); (vii) antiepileptics: carbamazepine (CBZ). The physicochemical properties of the target PPCPs are documented in Table S1.

All the chemicals used were of analytical grade unless stated otherwise. The PPCPs used for analysis were purchased from Aladdin (Shanghai, China) and Macklin (Shanghai, China). Three internal standards ($\text{CAF-}^{13}\text{C}_3$, $\text{SMN-}^{13}\text{C}_6$, and OFL-D_3) were obtained from Bepure (China, Beijing). Citric acid, ethylene glycol, $\text{SnCl}_4 \cdot 5\text{H}_2\text{O}$, SbCl_3 , La_2O_3 , ethanol, ascorbic acid, $\text{Na}_2\text{-EDTA}$, HPLC-grade MeOH, and formic acid were supplied by Aladdin (China). Milli-Q water (18.2 M Ω /cm) was used for preparing all the solutions in this experiment. Titanium meshes were purchased from Hebei Anheng (China). Commercial ceramic membrane was purchased from Ceraflo (Singapore).

2.2. Fabrication of Electrochemical Ceramic Membrane Module

A Ti/SnO₂-Sb-La electrode using titanium mesh (pore size = 170 μm , dimension = 6 cm \times 8 cm) as a substrate was prepared by the sol-gel method [20,25]. Briefly, the raw titanium mesh was degreased in 10 wt% NaOH for 60 min, rinsed with distilled water twice, and then etched in boiling 10 wt% oxalic acid for 30 min, followed by rinsing twice again. The precursor solution was prepared by dissolving $\text{SnCl}_4 \cdot 5\text{H}_2\text{O}$: SbCl_3 : La_2O_3 with the molar ratio 9:1:0.1 into a solution containing citric acid and ethylene glycol with the molar ratio 140:30. Finally, the titanium mesh was coated with the

solution prepared above, dried at 120 °C, and heated at 450 °C for 10 min. This coating and heating process was repeated 10 times, followed by heating at 500 °C for 2 h.

The electrochemical ceramic membrane module (effective filtration area 96 cm²) was assembled by the following steps (shown in Figure 1). In brief, a pristine titanium mesh was installed vertically in the middle of a polyvinyl chloride (PVC) frame (dimension = 6 cm × 8 cm × 2 cm) and served as the cathode, and then two pieces of Ti/SnO₂-Sb-La electrode were fixed on both sides of this frame to serve as the anodes. The distance between the anode and cathode was set at 1 cm, with the anodes and cathode connected to a DC power supply (Zhaoxing, China) via titanium wires. Finally, an electrochemical ceramic membrane module (effective filtration area = 96 cm²) was assembled by attaching two pieces of ceramic membrane onto the PVC frame via an epoxy resin adhesive.

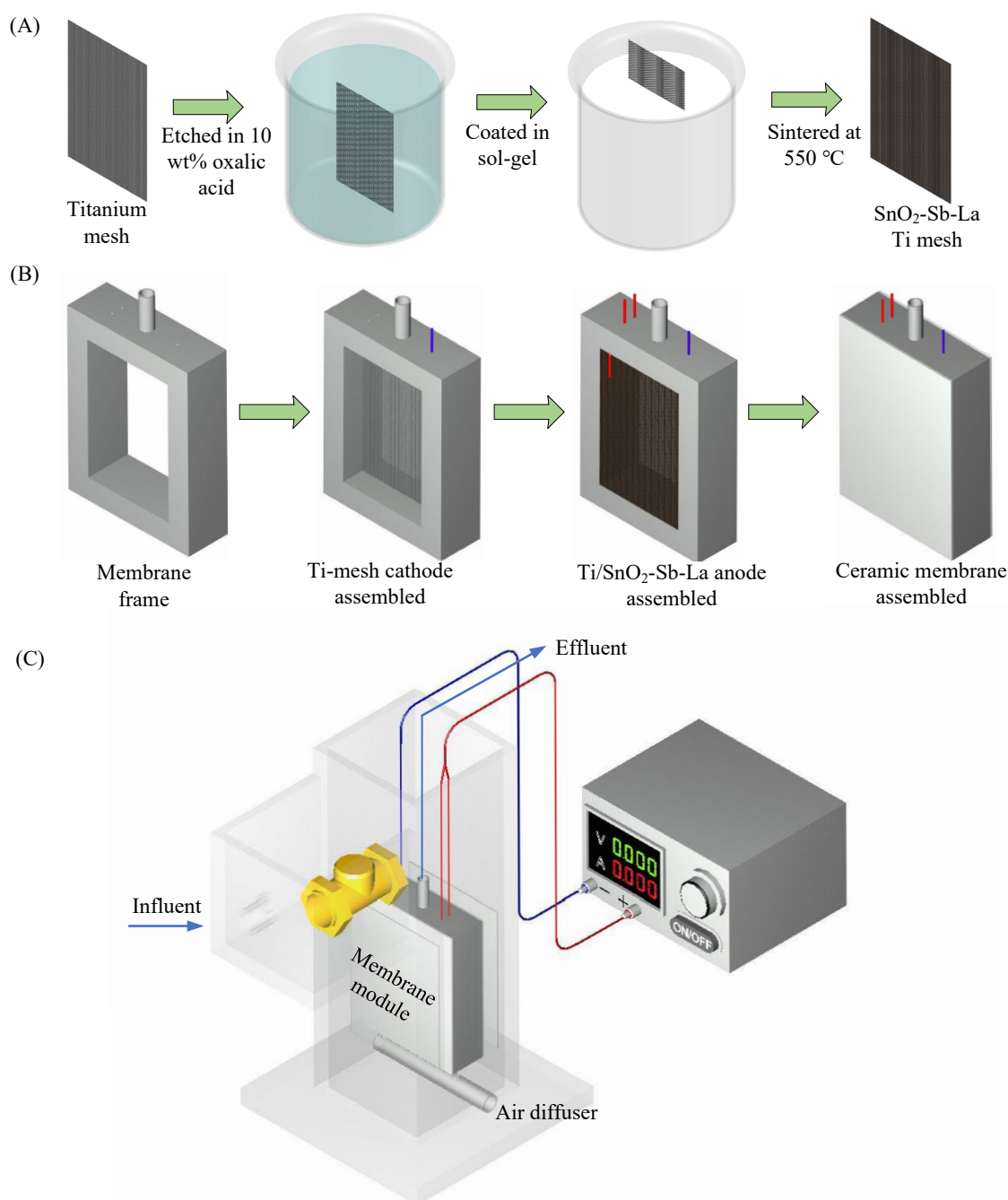


Figure 1. Schematic of (A) the fabrication process of the Ti/SnO₂-Sb-La electrode and (B) assembly of the electrochemical ceramic membrane module; (C) schematic of electrochemical ceramic membrane bioreactor (ECMBR) for wastewater treatment.

2.3. Experimental Setup and Operating Conditions

An ECMBR with an effective volume of 0.5 L was operated with an electric field (2 V/cm). The cell potential was 2 V and the average current intensity was 0.54 mA in the ECMBR. The inoculum sludge (~6.9 g/L) was collected from an MBR operated in Quyang Municipal Wastewater Treatment (WWTP). An air diffusion tube connected to an air pump was installed at the bottom of reactor with an aeration intensity of 100 m³/(m²·h) for supplying oxygen required by the microorganisms and scouring membrane surface for the fouling control. Peristaltic pumps (Lange, China) were used to withdraw the effluent from the membrane module at a constant membrane flux of 25 L/(m²·h). The hydraulic retention time (HRT) and sludge retention time (SRT) were set as 5 h and 30 days, respectively. Notably, the HRT in the permeate side of the membrane module (where electro-oxidation occurs) was 0.48 h. The sludge concentrations in ECMBR and CMBR were 5.54 ± 1.63 g/L and 5.40 ± 1.54 g/L, with no significant difference between them ($p > 0.05$). The intermittent operation mode—i.e., 10 min filtration, 2 min pause—was used for mitigating the membrane fouling. The membrane module was cleaned by 0.5% NaOCl solution when the trans-membrane pressure reached about 30 kPa. Wastewater from Quyang WWTP, Shanghai, China, was used as the feed water for the ECMBR. A conventional MBR (CMBR) was also operated with the same operating conditions but without an electric field, and was used as a control for comparison.

2.4. Analytical Methods

2.4.1. Membrane Characterization

Scanning electron microscope (SEM) and energy dispersive mapping (EDS) (S4800, Hitachi, Tokyo, Japan) were applied to observe the surface morphologies and elemental distribution of the Ti/SnO₂-Sb-La electrode. Linear sweep voltammetry (LSV) and electrochemical impedance spectroscopy (EIS) measurements were used to characterize the electrochemical properties of both the Ti/SnO₂-Sb-La electrode and pristine titanium mesh in a three-electrode system using an electrochemical workstation (CHI 660D, Shanghai Chenhua Co. Ltd., Shanghai, China). The average pore size of the ceramic membrane was determined by the bubble point method. The water contact angle of the membrane was measured by the sessile drop method. The water permeability was measured using a filtration cell under a constant pressure of 3 kPa.

2.4.2. Analysis of PPCPs

Solid phase extraction-ultra performance liquid chromatography-tandem mass spectrometry (SPE-UPLC-MS/MS) was used to determine the concentrations of PPCPs [10,26]. Detailed information about the analytical method is provided in Section S1 and Table S2. Briefly, samples were collected in a pre-cleaned amber glass bottle, followed by filtration through glass microfiber filters (0.7 µm, Whatman, UK) at a pH adjusted to 3.0 with 40% H₂SO₄. After adding 1 mL 25 g/L of ascorbic acid, 0.1 g of Na₂EDTA, and internal standards, the samples were extracted by flowing past a pre-conditioned HLB cartridge (500 mg/6 mL CNW). Then, the cartridges were rinsed by 5 mL 5% (*v/v*) of methanol aqueous and 5 mL of Milli-Q water, dried under vacuum for 10 min, and eluted by 10 mL of MeOH. Finally, the eluate was collected with a 10 mL glass tube, dried under a stream of N₂ in a 40 °C water bath, and adjusted to 1 mL with 40% methanol aqueous. The resulting extract was filtered through 0.2 µm polyether sulfone (PES) filters for a UPLC-MS/MS analysis. The recovery rates of the PPCPs ranged from 72% to 134% based on the detected concentration and the original spiked concentration [27].

2.4.3. Microbial Community Analysis

Sludge samples in ECMBR and CMBR were collected at 0 day (start-up) and 100 days (the end of the operation). The samples were sent to Majorbio (Shanghai, China) for sequencing on an Illumina Miseq platform using procedures presented in Section S2. Flash was used to overlap the paired-end reads after quality filtering conducted on Trimmomatic using the Sliding Window approach. An

identity threshold of 0.97 was used to cluster the sequences into different operational taxonomic units (OTUs) using UPARSE (version 7.1, <http://drive5.com/uparse/>), and chimeric sequences were identified and removed using UCHIME. The rarefaction curves, Chao, Shannon index, and Good's Coverage were determined by MOTHUR according to the standard procedures [28]. The taxonomy of each 16S rRNA gene sequence from the OTUs was analyzed by the RDP Classifier (<http://rdp.cme.msu.edu/>) and unite pipeline, respectively, with a confidence threshold of 70%. A microbial diversity analysis was performed using the Majorbio I-Sanger Cloud Platform (www.i-sanger.com).

2.4.4. Other Items

The chemical oxygen demand (COD) and ammonium ($\text{NH}_4^+\text{-N}$) in the influents and effluents and the mixed liquor suspend solids (MLSS) in the system were measured according to the Standard method (APHA, 2012). The trans-membrane pressure was determined by a mercury manometer. A Pearson correlation analysis was used to test the significance of difference among the results, and $p < 0.05$ is considered to be significantly different.

3. Results and Discussion

3.1. Characterization of Membrane and Electrodes

As shown in the SEM image of the Ti/SnO₂-Sb-La electrode (Figure 2A), the pre-treated titanium mesh was uniformly covered by an SnO₂-Sb-La layer. EDS mapping (Figure 2B) indicates that Sn, Sb, and La elements were present on the electrode surface, confirming the successful coating of the SnO₂-Sb-La layer. The anodic polarization potential of the Ti/SnO₂-Sb-La anode was close to 2.0 V, while the cathodic polarization potential of the titanium mesh was near −1.8 V based on an LSV analysis (Figure 2C). The diameter of the semicircle (Figure 2D) was defined as the charge-transfer resistance (RCT) of the electrodes [25]. The RCT of the Ti/SnO₂-Sb-La electrode and the titanium cathode was 176.9 Ω and 199.4 Ω , respectively. The average pore size of the ceramic membrane was 0.8 μm (Figure S1). The average pure water permeability of the conductive membrane was $331.7 \pm 6.2 \text{ L}/(\text{m}^2 \cdot \text{h} \cdot \text{kPa})$ (Figure S2), and the water contact angle was $37.5^\circ \pm 4.7^\circ$ (Figure S3). The SnO₂-Sb layer can improve the electrochemical efficiency for the decomposition of organic pollutants, and the doped rare earth elements La can mitigate the drawback of the short service life of the SnO₂-Sb electrodes [29,30]. The above-mentioned results showed that the electrodes had favorable electrochemical properties which could be incorporated into the electrochemical membrane module.

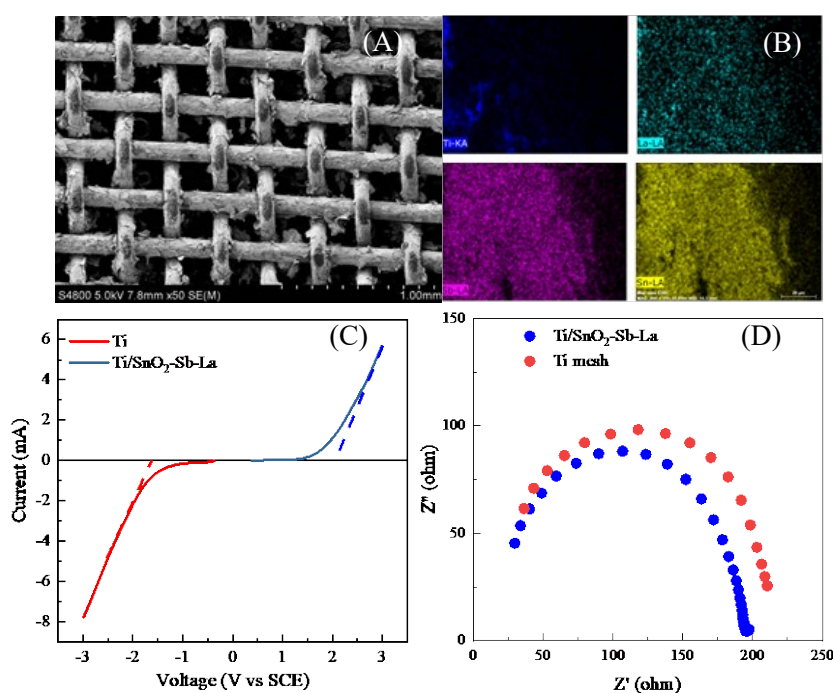


Figure 2. (A) SEM image and (B) EDS mapping of the Ti/SnO₂-Sb-La electrode; (C) linear sweep voltammetry (LSV) and (D) Nyquist plot of electrochemical impedance spectroscopy (EIS) of Ti/SnO₂-Sb-La electrode in a 5 mM Na₂SO₄ solution.

3.2. Performance of MBR Systems

The two reactors, operated in parallel, were used for the treatment of real wastewater. Figure 3A,B illustrate the removal performance of COD and NH₄⁺-N in the ECMBR and CMBR systems. The removal efficiency of the COD in the ECMBR was $87.7\% \pm 6.9\%$, which was similar to that in the CMBR ($88.7 \pm 6.7\%$) ($p > 0.05$). Similarly, the NH₄⁺-N removal efficiency ($98.3 \pm 1.5\%$) in the ECMBR also had no significant difference compared to that in the CMBR ($98.2 \pm 2.0\%$) ($p > 0.05$). The results showed that the presence of electric field had no adverse effects on the removal of the COD and ammonium, because (i) the electric field (2 V/cm) was relatively low [28,31] and (ii) the anodes and cathode were built in the electrochemical ceramic membrane module.

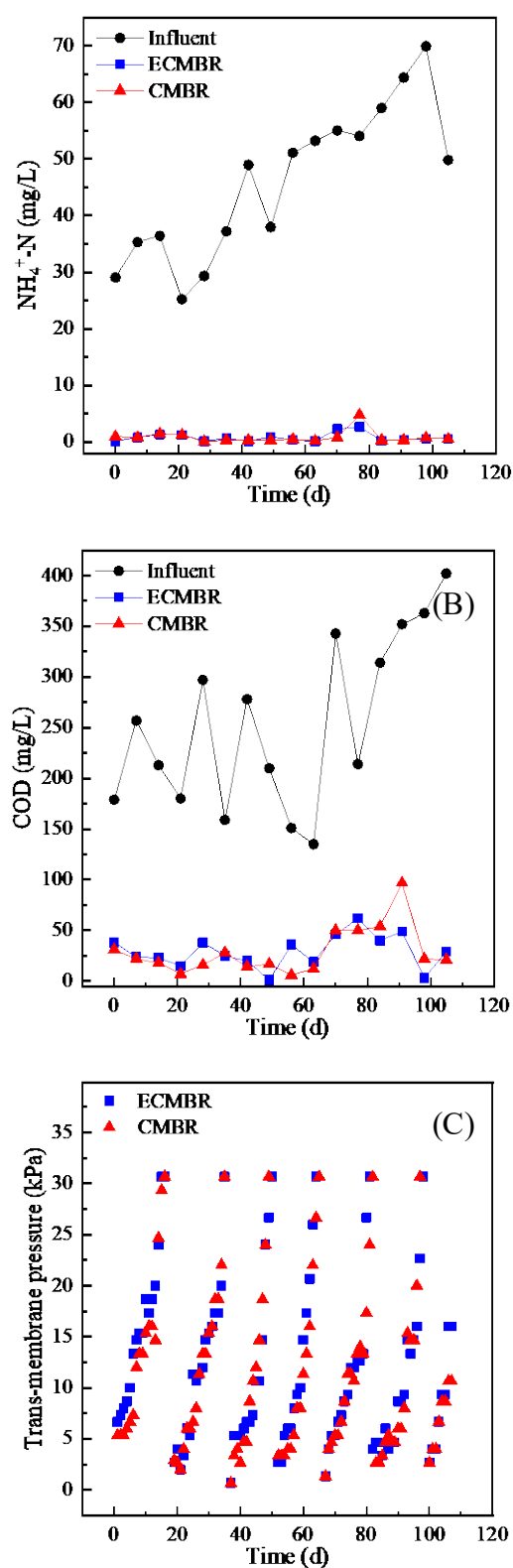


Figure 3. Performance of the MBR systems. (A) NH_4^+-N and (B) COD removal in ECMBR and conventional MBR (CMBR); (C) the evolution of trans-membrane pressure in the two MBRs.

The evolutions of trans-membrane pressure in the two MBRs are illustrated in Figure 3C. It can be observed that the trans-membrane pressure increase rates were almost the same (1.97 ± 0.20

kPa/day for ECMBR and 1.97 ± 0.19 kPa/day for CMBR). It showed that the presence of an electric field did not affect the membrane fouling rate. This result is different from that reported in literature [25,31,32], which is mainly associated with the location of the electrodes. In our study, built-in electrodes were used with the objective of the electrocatalytic oxidation of residual PPCPs after biodegradation. Therefore, the electrochemical effects could not well utilized for controlling the surface fouling of the ceramic membranes.

3.3. Occurrence and Removal of PPCPs

The concentrations of 24 kinds of PPCPs detected in the influent are listed in Table S3. In the influent, the most abundant PPCP was CAF, with concentrations in the range of 12,127.6–19,273.7 ng/L, which has also been reported to be frequently detected at the $\mu\text{g/L}$ level in municipal wastewater in China [26,33] and worldwide—e.g., in the USA [34] and Spain [35]. FQs were the dominant antibiotic in the influent, with a high concentration (3926.8–5969.2 ng/L), followed by MLs (417.8–4703.8 ng/L) and SAs (632.2–3576.6 ng/L). Two kinds of pharmaceuticals—antiepileptic CBZ (119.7–473.3 ng/L) and dihydrofolate reductase inhibitor TMP (194.9–552.8 ng/L)—were also detected in the influent. It was also found that OFL and MET were the predominant pharmaceuticals, with median concentrations of 3540.2 and 3609.7 ng/L, respectively. Moreover, SMX, SDZ, STZ, CIP, NOR, CLA, ROX, AZN, TIA, and TMP were also abundant PPCPs in the influent, with median concentrations higher than 200 ng/L. The concentrations of most PPCPs are in agreement with the range reported in the literature [10,33,36–38], while the concentration of MET is two times higher than the highest values reported previously [33,38], possibly due to several hospitals located in the service area of the WWTP.

The removal efficiencies of seven groups of PPCPs in ECMBR and CMBR are shown in Figure 4A (the sum of all the PPCP concentrations in each group). In general, the ECMBR enhanced the removal of PPCPs compared to CMBR. For FQs, the median removal efficiencies in ECMBR and CMBR were 82.8% and 52.9%, respectively. The ECMBR also achieved higher removal efficiencies of β -blockers (24.6%) and SAs (41.0%) compared to β -blockers (4.6%) and SAs (36.4%) on average in CMBR. Although the removal of MLs was not favorable in the two reactors, the ECMBR exhibited a slightly higher removal of MLs. For CAF, as a purine alkaloid, the CMBR had already achieved a high removal efficiency and the electrochemical oxidation in the ECMBR could not further degrade the CAF. The microorganisms enriched in activated sludge, such as pseudomonas, can effectively remove CAF by over 90% from wastewater [39]. In contrast, although TMP was not efficiently degraded in CMBR due to its antibiotic nature [40], the ECMBR significantly enhanced the removal of TMP to 66.5% compared to 15.6% in the CMBR. Both the ECMBR and the CMBR had low removal efficiencies for CBZ, indicating its resistance to both biotransformation and electrochemical oxidation [41].

For further elucidating the removal efficiencies of each PPCP, the seven groups were analyzed down to each PPCP level—i.e., 24 kinds of PPCPs in total. The removal efficiencies of 24 kinds of PPCPs in ECMBR and CMBR are shown in Figure 4B,C. The removal efficiency of the target PPCPs differs significantly due to their structural and/or physicochemical characteristics [33]. The removal efficiencies of FQs ranged from high to low: OFL > LOM > ENR > NOR > CIP, with efficiencies 63.0%, 41.8%, 28.3%, 12.3%, 6.4% in the CMBR and 92.4%, 47.6%, 48.0%, 34.3%, 32.1% in the ECMBR, respectively. It is obvious that the removal efficiency of FQs was enhanced by the electric field. The carboxyl group might facilitate the sorption of FQs [42,43] to the anodes for further electrocatalytic oxidation. Furthermore, the removal performance might be also dependent on their own structural features. The removal efficiencies of OFL and NOR were improved by 29.3% and 27.9% due their relatively simple structure in the ECMBR compared to the CMBR. The similar structure of CIP and ENR, both of which have cyclopropane rings, results in the similar enhancement with 19.8% and 19.7% in the ECMBR [44]. LOM, containing the -F group, has a strong stability, and the presence of the electric field only increased its removal by 5.8% on average.

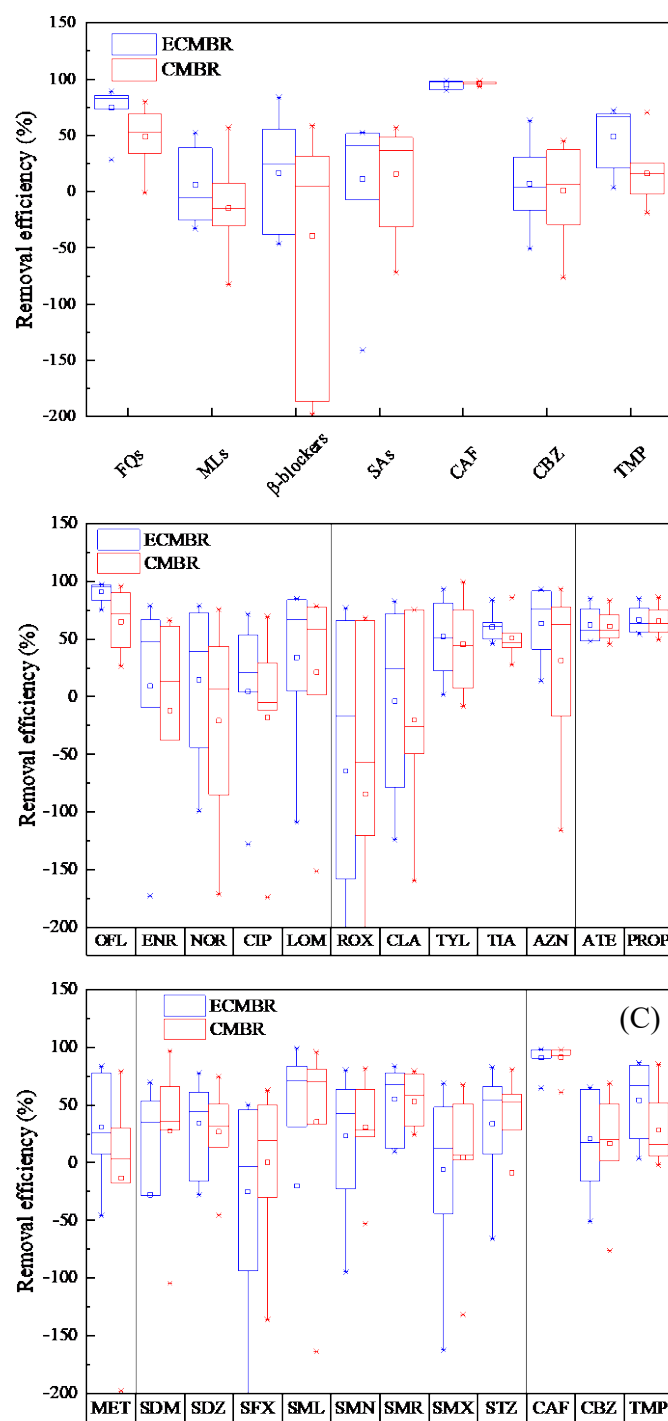


Figure 4. (A) Removal efficiencies of 7 groups of pharmaceutical and personal care products (PPCPs) in the ECMBR and CMBR. In each group, the sum of all the PPCP concentrations is regarded as the concentration of the group. Removal efficiencies of target PPCPs in the ECMBR and CMBR: (B) fluoroquinolones (FQs), MLs, and b-blockers; (C) SAs, CAF, CBZ, and TMP.

The removal efficiencies of MLs, a class of antibiotics with 12–16 carbon lactone rings in their molecular structure, were improved clearly by the electrochemical oxidation in the ECMBR. In this study, the median removal efficiencies of CLA and ROX were enhanced by 16.3% and 37.9%, respectively, with the introduction of an electric field, while the values of AZN, TYL, and TIA were increased slightly (5.4%, 5.8%, 6.6%, respectively). In view of their structural features (CLA and ROX with 14 carbon lactone rings, AZN with 15 carbon lactone rings, and TYL and TIA with 16 carbon lactone rings), a larger carbon lactone ring make it harder to degrade by electrochemical oxidation in

the ECMBR. For β -blockers, PROP and ATE exhibited a high resistance to electrochemical oxidation due to the presence of phenyl and amide groups, while the removal efficiency of MET was increased from 3.4% to 23.6% in the ECMBR [45].

For SAs, the ECMBR achieved slightly enhanced removal efficiencies for most kinds of SAs except SDM and SFX—for instance, SDZ (42.5% in ECMBR vs. 31.8% in CMBR), SML (68.1% vs. 61.8%), SMN (32.1% vs. 25.4%), SMR (66.5% vs. 53.9%), SMX (8.20% vs. 5.56%), and STZ (60.2% vs. 52.3%). A Pearson correlation analysis showed that the enhancement of SA degradation had negative correlations with $\log K_{ow}$ ($r = -0.808$, $p < 0.05$), indicating that the SAs with a high hydrophilicity facilitated the degradation by electrooxidation in the ECMBR. The mechanisms lying behind need further investigation. Overall, the ECMBR system significantly improved the removal efficiency of most of the PPCPs in this study with a slight increase in energy consumption (1.08×10^{-2} kWh/m³), indicating its great potential for industrial application.

3.4. Microbial Community Analysis

Illumina Miseq was used to analyze the microbial communities in ECMBR and CMBR at 0 day (Inoculum) and 100 days. After overlapping and quality control, 229,399 sequence amplicons with an average length of 416.47 bp in the V3-V4 region were obtained. The sampling coverage for these three samples is above 0.99 (Table S4), indicating that Illumina Miseq sequencing was able to detect most of the OTUs in this study [46]. The OTUs were clustered to 964 (ECMBR) and 853 (CMBR) at a distance of 3%. The total number of OTUs estimated by the Chao1 estimator was 1112 (ECMBR) and 1014 (CMBR) at a 3% distance, suggesting that the ECMBR had a higher microbial richness than CMBR due to the introduction of the electric field. The ECMBR also exhibited a higher microbial diversity than the CMBR, with a higher Shannon diversity index (5.08 in ECMBR vs 4.59 in CMBR).

As illustrated in Figure 5, the ECMBR in general had similar microbial structures to the CMBR. At the phylum level, 10 phyla accounted for over 99.9% of the abundance of the microbial community in these samples. Compared to the inoculum, the relative abundance of *Proteobacteria* in both the ECMBR and the CMBR increased and dominated microbial communities in the MBRs. The relative abundance of *Proteobacteria* in the ECMBR was 57%, slightly lower than that in the CMBR (60%). The relative abundance of *Actinobacteria* and *Chloroflexi* was decreased in both of the MBRs; however, the ECMBR always had a higher abundance (10% and 7%, respectively) compared to the CMBR (7% and 5%, respectively). The relative abundance of *Bacteroidetes* was maintained at around 14% in the ECMBR, while it increased to 16.7% in the CMBR. To further understand the evolutions of microbial communities in both MBRs, two predominant phyla were chosen to analyze their compositions at the class level (Figure 5B,C). In general, the ECMBR showed similar microbial communities to CMBR (Figure 5B,C), suggesting that a low electric field would not significantly affect the microbial community in the ECMBR. The enhanced removal of PPCPs should be potentially attributed to the incorporation of electrochemical oxidation in the MBR.

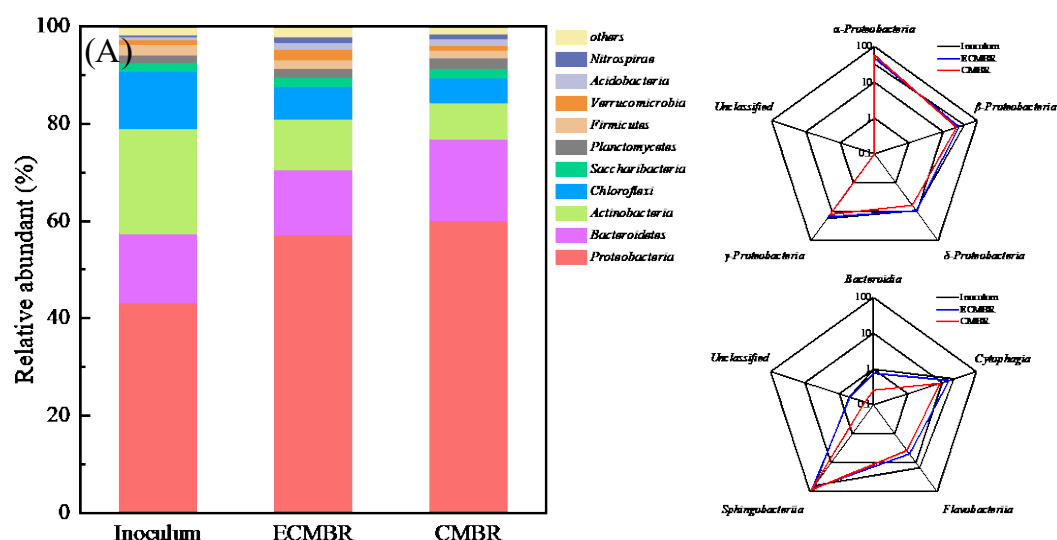
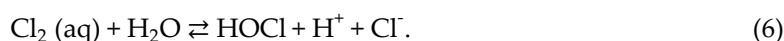


Figure 5. (A) Relative abundance of the bacteria of Inoculum, CMBR, and ECMBR at the phylum level. Phyla making up less than 0.1% are defined as “others”. (B,C) Relative abundance of the predominant phylogenetic groups of Inoculum, ECMBR, and CMBR at the class level. Relative abundance was calculated as the number of sequences affiliated that taxon divided by the total number of sequences per sample (%).

3.5. Mechanism for the Enhanced Removal of PPCPs in ECMBR

In the ECMBR, the PPCP degradation is mainly associated with oxidation by ROS (e.g., H_2O_2 and $\text{HO}\cdot$) and active chlorine during the electrochemical process (see Equations (1)–(6)) [28,47,48]. Equations (1)–(3) are anodic oxidation reactions, Equations (4) and (5) are cathodic reactions, and Equation (6) is initiated in the bulk solution. The ROS were measured in the electrochemical reactor, with the quantity of ROS 98.1 times that of the control group (Figure S4). The concentration of H_2O_2 in the ECMBR system was $160.2 \pm 13.3 \mu\text{mol/L}$, and the concentration of Cl_T was $80.1 \pm 0.85 \mu\text{mol/L}$ (Figure S4).



The enhanced degradation mechanism of PPCPs in the ECMBR system is shown in Figure 6, which is mainly attributed to: (i) the electrochemical membrane module can intercept large particles and colloids by the physical retention of ceramic microfiltration membrane, thereby protecting the electrodes against fouling and prolonging the serve life of the electrodes; (ii) the activated sludge could degrade most of the biodegradable dissolved organic matter and residual organic pollutants like PPCPs, which are difficult to biodegrade, and enter the electrochemical ceramic membrane module through the membrane filtration; (iii) oxidants such as Cl_T (HOCl/OCl^-) and ROS (H_2O_2 and $\text{HO}\cdot$) produced by the electrodes can oxidize PPCPs in the membrane compartment, thereby achieving a higher electrochemical efficiency.

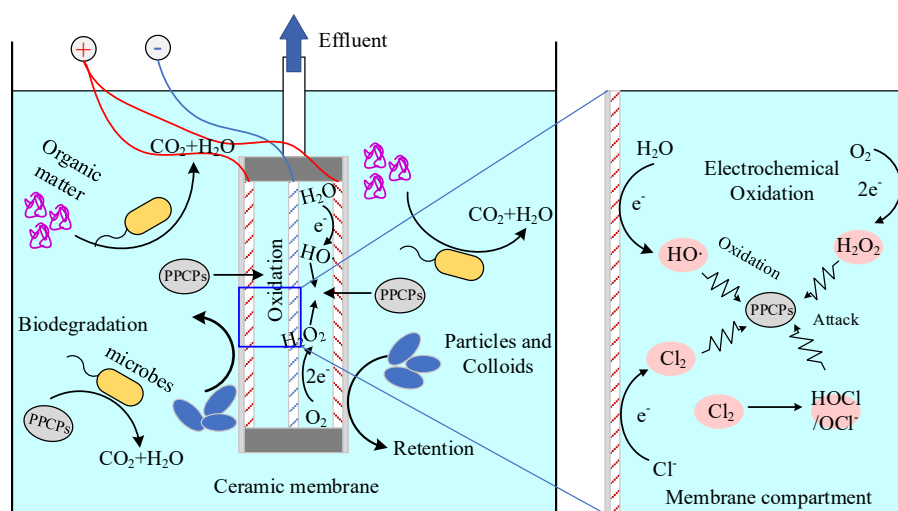


Figure 6. Schematic of the mechanisms for PPCP removal in the ECMBR.

4. Conclusions

An ECMBR with built-in electrodes was developed for removing PPCPs from real wastewater. The results demonstrated that in the presence of an electric field (2 V/cm), the ECMBR could enhance the removal efficiencies of most targeted PPCPs without having adverse impacts on conventional pollutant removal and membrane fouling. Furthermore, the exertion of the electric field did not cause significant changes in the microbial communities, suggesting that the enhanced removal of PPCPs should be mainly attributed to the electrochemical oxidation by the built-in electrodes in the ECMBR. The results highlight the potential of using ECMBR for removing PPCPs from contaminated water. Further investigation on the removal performance of PPCPs using a pilot-scale ECMBR is needed for promoting its applications in the advanced treatment of wastewater.

Supplementary Materials: The following are available online at www.mdpi.com/2073-4441/12/6/1838/s1. Figure S1: Average pore size of ceramic membrane, Figure S2: Average pure water permeability of the conductive membrane, Figure S3: Water contact angle of ceramic membrane, Figure S4: (a) ROS production in the batch tests ($n = 3$); (b) Concentrations of H_2O_2 in CMBR and ECMBR in the batch tests ($n = 3$); (c) Concentrations of Cl^- in CMBR and ECMBR in the batch tests ($n = 3$), Table S1: physical-chemical properties and molecular structures of target PPCPs, Table S2: Operational parameters of tandem MS and LOQs of target PPCPs in wastewater, Table S3: Concentrations of target PPCPs in Influent of EMBR and CMBR, Table S4: Richness and diversity estimators of the bacteria phylotypes in the two MBR systems.

Author Contributions: All authors have read and agree to the published version of the manuscript. Conceptualization, Z.W.; methodology, K.Q., Q.L., M.C. and M.L.; investigation, K.Q. and R.D.; resources, Z.W.; data curation, K.Q.; writing—original draft preparation, K.Q.; writing—review and editing, K.Q., M.C., R.D. and Z.W.; supervision, Z.W.; project administration, M.C. and Z.W.; funding acquisition, Z.W. All authors have read and agreed to the published version of the manuscript.

Funding: This research was funded by the National Natural Science Foundation of China (Grant 51838009 & 52041002).

Conflicts of Interest: The authors declare no conflict of interest.

References

1. Klein, E.Y.; van Boeckel, T.P.; Martinez, E.M.; Pant, S.; Gandra, S.; Levin, S.A.; Goossens, H.; Laxminarayan, R. Global increase and geographic convergence in antibiotic consumption between 2000 and 2015. *Proc. Natl. Acad. Sci. USA* **2018**, *115*, E3463–E3470, doi:10.1073/pnas.1717295115.
2. Wilkinson, J.; Hooda, P.S.; Barker, J.; Barton, S.; Swinden, J. Occurrence, fate and transformation of emerging contaminants in water: An overarching review of the field. *Environ. Pollut.* **2017**, *231*, 954–970, doi:10.1016/j.envpol.2017.08.032.

3. Tran, N.H.; Chen, H.; Reinhard, M.; Mao, F.; Gin, K.Y.-H. Occurrence and removal of multiple classes of antibiotics and antimicrobial agents in biological wastewater treatment processes. *Water Res.* **2016**, *104*, 461–472, doi:10.1016/j.watres.2016.08.040.
4. Daughton, C.G.; Ruhoy, I.S. Environmental footprint of pharmaceuticals: The significance of factors beyond direct excretion to sewers. *Environ. Toxicol. Chem.* **2009**, *28*, 2495–2521, doi:10.1897/08-382.1.
5. Kümmerer, K. Antibiotics in the aquatic environment—A review—Part I. *Chemosphere* **2009**, *75*, 417–434, doi:10.1016/j.chemosphere.2008.11.086.
6. Braund, R.; Peake, B.M.; Shieffebien, L. Disposal practices for unused medications in New Zealand. *Environ. Int.* **2009**, *35*, 952–955, doi:10.1016/j.envint.2009.04.003.
7. Vatovec, C.; van Wagoner, E.; Evans, C. Investigating sources of pharmaceutical pollution: Survey of over-the-counter and prescription medication purchasing, use, and disposal practices among university students. *J. Environ. Manag.* **2017**, *198*, 348–352, doi:10.1016/j.jenvman.2017.04.101.
8. Cheng, D.; Ngo, H.H.; Guo, W.; Liu, Y.; Chang, S.W.; Nguyen, D.D.; Nghiem, L.D.; Zhou, J.; Ni, B. Anaerobic membrane bioreactors for antibiotic wastewater treatment: Performance and membrane fouling issues. *Bioresour. Technol.* **2018**, *267*, 714–724, doi:10.1016/j.biortech.2018.07.133.
9. Vikesland, P.J.; Pruden, A.; Alvarez, P.J.J.; Aga, D.; Bürgmann, H.; Li, X.; Manaia, C.M.; Nambi, I.; Wigginton, K.; Zhang, T.; et al. Toward a Comprehensive Strategy to Mitigate Dissemination of Environmental Sources of Antibiotic Resistance. *Environ. Sci. Technol.* **2017**, *51*, 13061–13069, doi:10.1021/acs.est.7b03623.
10. Ben, W.; Zhu, B.; Yuan, X.; Zhang, Y.; Yang, M.; Qiang, Z. Occurrence, removal and risk of organic micropollutants in wastewater treatment plants across China: Comparison of wastewater treatment processes. *Water Res.* **2018**, *130*, 38–46, doi:10.1016/j.watres.2017.11.057.
11. Oberoi, A.S.; Jia, Y.; Zhang, H.; Khanal, S.K.; Lu, H. Insights into the Fate and Removal of Antibiotics in Engineered Biological Treatment Systems: A Critical Review. *Environ. Sci. Technol.* **2019**, *53*, 7234–7264, doi:10.1021/acs.est.9b01131.
12. Huang, X.; Xiao, K.; Shen, Y. Recent advances in membrane bioreactor technology for wastewater treatment in China. *Front. Environ. Sci. Eng. China* **2010**, *4*, 245–271, doi:10.1007/s11783-010-0240-z.
13. Ma, J.; Dai, R.; Chen, M.; Khan, S.J.; Wang, Z. Applications of membrane bioreactors for water reclamation: Micropollutant removal, mechanisms and perspectives. *Bioresour. Technol.* **2018**, *269*, 532–543, doi:10.1016/j.biortech.2018.08.121.
14. Guinea, E.; Brillas, E.; Centellas, F.; Cañizares, P.; Rodrigo, M.A.; Sáez, C. Oxidation of enrofloxacin with conductive-diamond electrochemical oxidation, ozonation and Fenton oxidation. A comparison. *Water Res.* **2009**, *43*, 2131–2138, doi:10.1016/j.watres.2009.02.025.
15. Michael, I.; Rizzo, L.; McArdell, C.S.; Manaia, C.M.; Merlin, C.; Schwartz, T.; Dagot, C.; Fatta-Kassinos, D. Urban wastewater treatment plants as hotspots for the release of antibiotics in the environment: A review. *Water Res.* **2013**, *47*, 957–995, doi:10.1016/j.watres.2012.11.027.
16. Moreira, F.C.; Soler, J.; Alpendurada, M.F.; Boaventura, R.A.R.; Brillas, E.; Vilar, V.J.P. Tertiary treatment of a municipal wastewater toward pharmaceuticals removal by chemical and electrochemical advanced oxidation processes. *Water Res.* **2016**, *105*, 251–263, doi:10.1016/j.watres.2016.08.036.
17. Rizzo, L. Bioassays as a tool for evaluating advanced oxidation processes in water and wastewater treatment. *Water Res.* **2011**, *45*, 4311–4340, doi:10.1016/j.watres.2011.05.035.
18. Wang, W.; Lu, Y.; Luo, H.; Liu, G.; Zhang, R.; Jin, S. A microbial electro-fenton cell for removing carbamazepine in wastewater with electricity output. *Water Res.* **2018**, *139*, 58–65, doi:10.1016/j.watres.2018.03.066.
19. Dirany, A.; Sirés, I.; Oturan, N.; Özcan, A.; Oturan, M.A. Electrochemical Treatment of the Antibiotic Sulfachloropyridazine: Kinetics, Reaction Pathways, and Toxicity Evolution. *Environ. Sci. Technol.* **2012**, *46*, 4074–4082, doi:10.1021/es204621q.
20. Zheng, J.; Wang, Z.; Ma, J.; Xu, S.; Wu, Z. Development of an Electrochemical Ceramic Membrane Filtration System for Efficient Contaminant Removal from Waters. *Environ. Sci. Technol.* **2018**, *52*, 4117–4126, doi:10.1021/acs.est.7b06407.
21. Zheng, J.; Ma, J.; Wang, Z.; Xu, S.; Waite, T.D.; Wu, Z. Contaminant Removal from Source Waters Using Cathodic Electrochemical Membrane Filtration: Mechanisms and Implications. *Environ. Sci. Technol.* **2017**, *51*, 2757–2765, doi:10.1021/acs.est.6b05625.

22. Kong, D.; Liang, B.; Yun, H.; Cheng, H.; Ma, J.; Cui, M.; Wang, A.; Ren, N. Cathodic degradation of antibiotics: Characterization and pathway analysis. *Water Res.* **2015**, *72*, 281–292, doi:10.1016/j.watres.2015.01.025.
23. Pérez-Moya, M.; Graells, M.; Castells, G.; Amigó, J.; Ortega, E.; Buhigas, G.; Pérez, L.M.; Mansilla, H.D. Characterization of the degradation performance of the sulfamethazine antibiotic by photo-Fenton process. *Water Res.* **2010**, *44*, 2533–2540, doi:10.1016/j.watres.2010.01.032.
24. Antonin, V.S.; Santos, M.C.; Garcia-Segura, S.; Brillas, E. Electrochemical incineration of the antibiotic ciprofloxacin in sulfate medium and synthetic urine matrix. *Water Res.* **2015**, *83*, 31–41, doi:10.1016/j.watres.2015.05.066.
25. Fu, W.; Wang, X.; Zheng, J.; Liu, M.; Wang, Z. Antifouling performance and mechanisms in an electrochemical ceramic membrane reactor for wastewater treatment. *J. Membr. Sci.* **2019**, *570–571*, 355–361, doi:10.1016/j.memsci.2018.10.077.
26. Yuan, X.; Qiang, Z.; Ben, W.; Zhu, B.; Qu, J. Distribution, mass load and environmental impact of multiple-class pharmaceuticals in conventional and upgraded municipal wastewater treatment plants in East China. *Environ. Sci.: Processes Impacts* **2015**, *17*, 596–605, doi:10.1039/C4EM00596A.
27. Yuan, X.; Qiang, Z.; Ben, W.; Zhu, B.; Liu, J. Rapid detection of multiple class pharmaceuticals in both municipal wastewater and sludge with ultra high performance liquid chromatography tandem mass spectrometry. *J. Environ. Sci.* **2014**, *26*, 1949–1959, doi:10.1016/j.jes.2014.06.022.
28. Chen, M.; Xu, J.; Dai, R.; Wu, Z.; Liu, M.; Wang, Z. Development of a moving-bed electrochemical membrane bioreactor to enhance removal of low-concentration antibiotic from wastewater. *Bioresour. Technol.* **2019**, *293*, 122022.
29. Bi, Q.; Guan, W.; Gao, Y.; Cui, Y.; Ma, S.; Xue, J. Study of the mechanisms underlying the effects of composite intermediate layers on the performance of Ti/SnO₂-Sb-La electrodes. *Electrochim. Acta.* **2019**, *306*, 667–679, doi:10.1016/j.electacta.2019.03.122.
30. Zhu, F.-L.; Meng, Y.-S.; Huang, X.-Y. Electro-catalytic degradation properties of Ti/SnO₂-Sb electrodes doped with different rare earths. *Rare Met.* **2016**, *35*, 412–418, doi:10.1007/s12598-014-0397-x.
31. Huang, J.; Wang, Z.; Zhang, J.; Zhang, X.; Ma, J.; Wu, Z. A novel composite conductive microfiltration membrane and its anti-fouling performance with an external electric field in membrane bioreactors. *Sci. Rep.* **2015**, *5*, 1–8, doi:10.1038/srep09268.
32. Liu, H.; Zhang, G.; Zhao, C.; Liu, J.; Yang, F. Hydraulic power and electric field combined antifouling effect of a novel conductive poly(aminoanthraquinone)/reduced graphene oxide nanohybrid blended PVDF ultrafiltration membrane. *J. Mater. Chem. A* **2015**, *3*, 20277–20287, doi:10.1039/C5TA05306D.
33. Xue, W.; Wu, C.; Xiao, K.; Huang, X.; Zhou, H.; Tsuno, H.; Tanaka, H. Elimination and fate of selected micro-organic pollutants in a full-scale anaerobic/anoxic/aerobic process combined with membrane bioreactor for municipal wastewater reclamation. *Water Res.* **2010**, *44*, 5999–6010, doi:10.1016/j.watres.2010.07.052.
34. Hedgespeth, M.L.; Sapozhnikova, Y.; Pennington, P.; Clum, A.; Fairey, A.; Wirth, E. Pharmaceuticals and personal care products (PPCPs) in treated wastewater discharges into Charleston Harbor, South Carolina. *Sci. Total Environ.* **2012**, *437*, 1–9, doi:10.1016/j.scitotenv.2012.07.076.
35. Bueno, M.J.M.; Gomez, M.J.; Herrera, S.; Hernando, M.D.; Agüera, A.; Fernández-Alba, A.R. Occurrence and persistence of organic emerging contaminants and priority pollutants in five sewage treatment plants of Spain: Two years pilot survey monitoring. *Environ. Pollut.* **2012**, *164*, 267–273, doi:10.1016/j.envpol.2012.01.038.
36. Kasprzyk-Hordern, B.; Dinsdale, R.M.; Guwy, A.J. The removal of pharmaceuticals, personal care products, endocrine disruptors and illicit drugs during wastewater treatment and its impact on the quality of receiving waters. *Water Res.* **2009**, *43*, 363–380, doi:10.1016/j.watres.2008.10.047.
37. Radjenović, J.; Petrović, M.; Barceló, D. Fate and distribution of pharmaceuticals in wastewater and sewage sludge of the conventional activated sludge (CAS) and advanced membrane bioreactor (MBR) treatment. *Water Res.* **2009**, *43*, 831–841, doi:10.1016/j.watres.2008.11.043.
38. Vieno, N.; Tuhkanen, T.; Kronberg, L. Elimination of pharmaceuticals in sewage treatment plants in Finland. *Water Res.* **2007**, *41*, 1001–1012, doi:10.1016/j.watres.2006.12.017.
39. Quandt, E.M.; Hammerling, M.J.; Summers, R.M.; Otoupal, P.B.; Slater, B.; Alnahhas, R.N.; Dasgupta, A.; Bachman, J.L.; Subramanian, M.V.; Barrick, J.E. Decaffeination and Measurement of Caffeine Content by

- Addicted *Escherichia coli* with a Refactored N-Demethylation Operon from *Pseudomonas putida* CBB5. *ACS Synth. Biol.* **2013**, *2*, 301–307, doi:10.1021/sb4000146.
40. Moreira, F.C.; Garcia-Segura, S.; Boaventura, R.A.R.; Brillas, E.; Vilar, V.J.P. Degradation of the antibiotic trimethoprim by electrochemical advanced oxidation processes using a carbon-PTFE air-diffusion cathode and a boron-doped diamond or platinum anode. *Appl. Catal. B Environ.* **2014**, *160–161*, 492–505, doi:10.1016/j.apcatb.2014.05.052.
41. Subedi, B.; Kannan, K. Occurrence and fate of select psychoactive pharmaceuticals and antihypertensives in two wastewater treatment plants in New York State, USA. *Sci. Total Environ.* **2015**, *514*, 273–280, doi:10.1016/j.scitotenv.2015.01.098.
42. Dorival-García, N.; Zafra-Gómez, A.; Navalón, A.; González-López, J.; Hontoria, E.; Vílchez, J.L. Removal and degradation characteristics of quinolone antibiotics in laboratory-scale activated sludge reactors under aerobic, nitrifying and anoxic conditions. *J. Environ. Manag.* **2013**, *120*, 75–83, doi:10.1016/j.jenvman.2013.02.007.
43. Wang, L.; Qiang, Z.; Li, Y.; Ben, W. An insight into the removal of fluoroquinolones in activated sludge process: Sorption and biodegradation characteristics. *J. Environ. Sci.* **2017**, *56*, 263–271, doi:10.1016/j.jes.2016.10.006.
44. Jiang, C.; Ji, Y.; Shi, Y.; Chen, J.; Cai, T. Sulfate radical-based oxidation of fluoroquinolone antibiotics: Kinetics, mechanisms and effects of natural water matrices. *Water Res.* **2016**, *106*, 507–517, doi:10.1016/j.watres.2016.10.025.
45. Veloutsou, S.; Bizani, E.; Fytianos, K. Photo-Fenton decomposition of β -blockers atenolol and metoprolol; study and optimization of system parameters and identification of intermediates. *Chemosphere* **2014**, *107*, 180–186, doi:10.1016/j.chemosphere.2013.12.031.
46. Chen, M.; Zhang, X.; Wang, Z.; Wang, L.; Wu, Z. QAC modified PVDF membranes: Antibiofouling performance, mechanisms, and effects on microbial communities in an MBR treating municipal wastewater. *Water Res.* **2017**, *120*, 256–264, doi:10.1016/j.watres.2017.05.012.
47. Degaki, A.H.; Pereira, G.F.; Rocha-Filho, R.C.; Bocchi, N.; Biaggio, S.R. Effect of Specific Active Chlorine Species and Temperature on the Electrochemical Degradation of the Reactive Blue 19 Dye Using a Boron-Doped Diamond or DSA Anode in a Flow Reactor. *Electrocatalysis* **2014**, *5*, 8–15, doi:10.1007/s12678-013-0156-z.
48. Park, H.; Vecitis, C.D.; Hoffmann, M.R. Electrochemical Water Splitting Coupled with Organic Compound Oxidation: The Role of Active Chlorine Species. *J. Phys. Chem. C* **2009**, *113*, 7935–7945, doi:10.1021/jp810331w.

